ELSEVIER

Chemical Engineering Journal 139 (2008) 390–397

Chemical Engineering Journal

www.elsevier.com/locate/cej

A multi-phase AC arc discharge and its application in in-flight thermal treatment of raw glass powders

Y. Yao [a], M.M. Hossain [a], T. Watanabe [a,*], T. Matsuura [b], F. Funabiki [c], T. Yano [c]

[a] *Department of Environmental Chemistry and Engineering, Tokyo Institute of Technology, 4251-G1-22 Nagatsuda, Midori-ku, Yokohama 226-8502, Japan*
[b] *Industrial Technology Center of Fukui Prefecture, 61 Kawai-Washizuka, Fukui 910-0102, Japan*
[c] *Department of Chemistry and Materials Science, Tokyo Institute of Technology, 2-12-1-S7-4 Ookayama, Meguro-ku, Tokyo 152-8550, Japan*

Received 4 September 2007; received in revised form 26 October 2007; accepted 7 November 2007

Abstract

The in-flight melting technology with multi-phase alternating current (AC) arc was developed for the purpose of saving energy and shortening production cycle for glass industry. The 6-phase arc and 12-phase arc were used to investigate the in-flight melting behavior of soda-lime and alkali-free glass powders. Results showed that the vitrification degree of raw materials and the shrinkage of particle diameter increased with the increase of input power. The higher melting temperature and viscosity were responsible for the lower vitrification degree of alkali-free glass powders. Compared with 6-phase arc, 12-phase arc improved the vitrification degree of raw material for the longer residence time and higher plasma temperature under the same transformer current. The high vitrification degree achieved in short time indicated that the new in-flight melting technology with multi-phase ac arc would be a promising method for energy conservation in glass industry.

Keywords: Thermal plasmas; Multi-phase ac arc; In-flight melting; Glass production

1. Introduction

The glass industry has been using the typical siemens-type melters for the good performance of large-scale melting since 1860 [1]. The conventional method used for glass melting is the air–fuel firing technology, which is inefficient, time consuming and energy intensive. Especially, the melting and refining (removal of gas bubbles) process is the most energy intensive and time consuming in the whole technology. In addition, the usage of fossil fuel during the traditional technology brings more environmental responsibility due to the emissions of greenhouse gases like CO_2 and NO_x. Researchers have come up with a variety of partial solutions with more insulation, more efficient burner, and improved refractory and furnace designs [2–4]. Some researchers have tried to change the fuel source to increase the temperature and reduce the emissions by using oxygen instead of air in furnaces, other producers used electric boosting to hasten melting time and improve their processes [5,6]. Most of those improvements, however, have not changed the fundamental technology, only produce small energy savings. With the increase of usage of glass and the energy issue, it is crucial to develop a new high-efficiency glass melting technology with minimum energy consumption and emissions.

Thermal plasmas have received many attentions owing to its high chemical reactivity, easy and rapid generation of high temperature, high enthalpy to enhance the reaction kinetic, oxidation and reduction atmosphere in accordance with required chemical reaction as well as rapid quenching capability. The thermal plasmas have been widely applied to many fields because of these unique advantages, such as spray coating, extraction of metals, remelting and refining of metals or alloys, synthesis of advanced materials as well as treatment of toxic and hazardous wastes [7–12]. Among various kinds of thermal plasma reactors, arc plasma as the energy source with high energy efficiency has been using in the welding and cutting of metals, steelmaking, synthesis of nanoparticles and spheriodization of metal particles [13–15]. The valuable feature of an electric power system with more than three phases is that the instantaneous power is almost constant when the power source and its load are balanced [16–18]. The high temperature of arc plasma makes it possible to develop an energy saving and environment benign technology for glass melting.

* Corresponding author. Tel.: +81 45 924 5414; fax: +81 45 924 5414.
E-mail address: watanabe@chemenv.titech.ac.jp (T. Watanabe).

1385-8947/$ – see front matter © 2007 Elsevier B.V. All rights reserved.
doi:10.1016/j.cej.2007.11.016

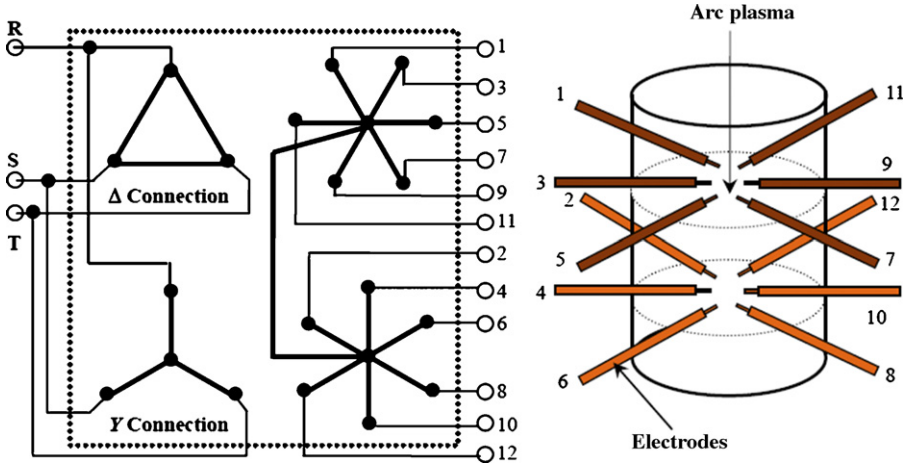

Fig. 1. Electrical circuit diagram of the transformers for converting from the 3-phase ac to the 12-phase ac.

In this study, an innovative glass melting technology with multi-phase alternating current (AC) arc was developed to melt granulated raw material during its flight time for the purpose of energy conservation and environmental protection. The vitrification, morphology, particle size distribution, and composition of powders were characterized by different analysis methods. Also, the effect of input power of arc on the in-flight melting behavior of two kinds of powders was investigated in the paper.

2. Experimental

The raw materials for soda-lime and alkali-free glass were prepared into granulated powders using the spray-drying method; the mean diameter was 51 and 80 μm, respectively. The porosities of raw materials of soda-lime and alkali-free glass were 73% and 72%, respectively. The target composition of soda-lime glass was $16Na_2O–10CaO–74SiO_2$ (wt%) made from Na_2CO_3, $CaCO_3$ and SiO_2, the composition of alkali-free glass was $49SiO_2–15B_2O_3–10Al_2O_3–25BaO–1Sb_2O_3$ (wt%) prepared from SiO_2, H_3BO_3, Al_2O_3, $BaCO_3$ and Sb_2O_3.

The new type of arc plasma reactor with multi-phase (6 or 12) AC discharge has been developed to get stable and continuous arc by the transformers for converting from the 3-phase AC to the multi-phase AC, as shown in Fig. 1. The single-phase AC arc welding transformers (DAIHEN B-300) were used to realize the

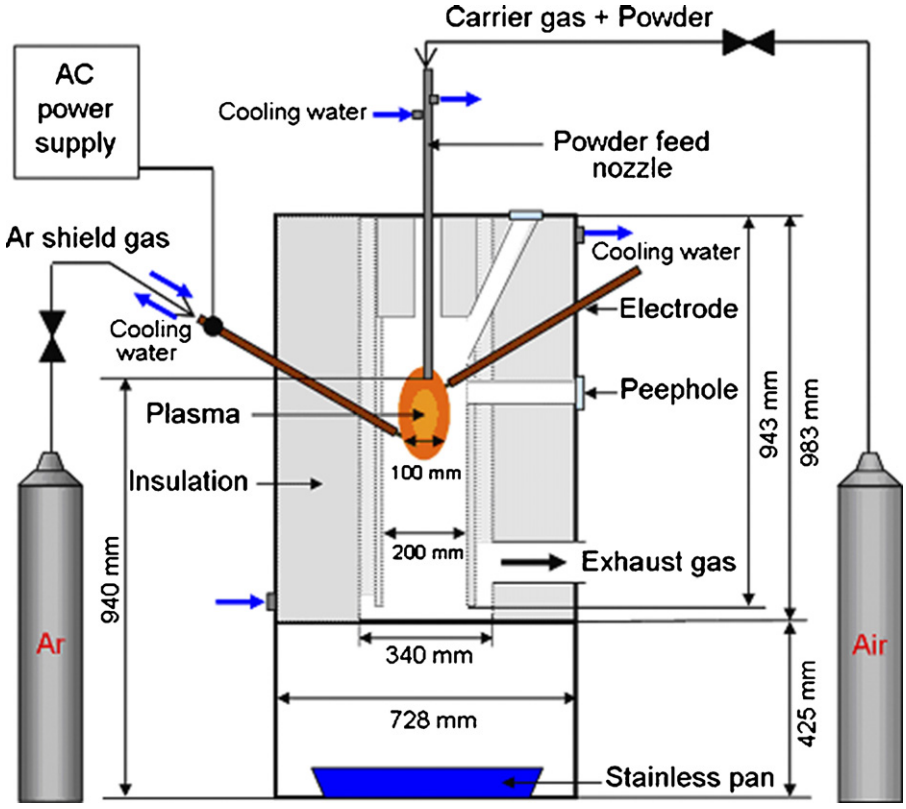

Fig. 2. Schematic diagram of the experimental setup.

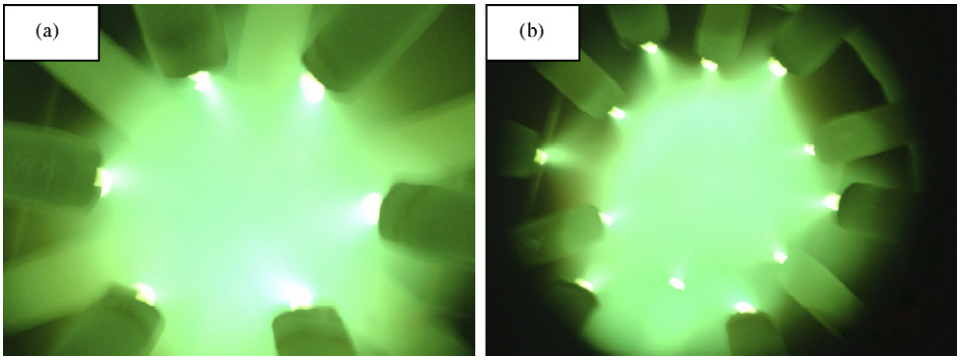

Fig. 3. Photographs of multi-phase arc plasma: (a) 6-phase arc and (b) 12-phase arc.

power supply for the generation of multi-phase arc. The input of the 3-phase power supply was connected to 200 V (50 Hz) commercial power lines. The primary coils of transformers were divided into two parts: one was the Δ connection and the other was the Y connection. The vector diagrams for converting from 3-phase to 12-phase were reported by Matsuura et al. [18]. The output lines from transformers were connected directly to the corresponding electrodes of the reactor.

The schematic diagram of experimental setup is shown in Fig. 2. It consisted of 12 electrodes, reaction chamber, powder feeder and AC power supply. The configuration of 12 electrodes was symmetrically arranged by the angle of 30°. Twelve electrodes were divided into two layers, upper six electrodes and lower six electrodes. The electrode material was tungsten (purity 99.9%) with 3.2 mm in diameter. The electrodes and the powder feeder nozzle were water cooled; argon gas (99.99%) was injected around the electrodes to prevent them from oxidation at the flow rate of 36 l/min. The set-up can be operated with 6-electrode discharge or 12-electrode discharge. Fig. 3 shows the generated arc plasma with 6-electrode discharge and 12-electrode discharge. In the experiments, the transformer current was set to 100, 125 and 150 A, corresponding to the input power of 22, 27 and 30 kW for 6-phase arc. Since the maximum input power is 52 kW for this setup, only two types of power 36 and 46 kW) for 12-phase arc can be generated at the input current of 100 and 125 A, respectively. The discharge voltage and current of each electrode were 30–45 V and 80–130 A, respectively. The diameter of arc plasma was about 100 mm; the distance between two layers of electrodes was 150 mm. The raw materials were injected into the arc plasma at the feed rate of 30 g/min with air carrier gas of 20 l/min by the powder feeder. The powders treated by multi-arc were quenched on the stainless steel pan at a distance of 920 mm below nozzle.

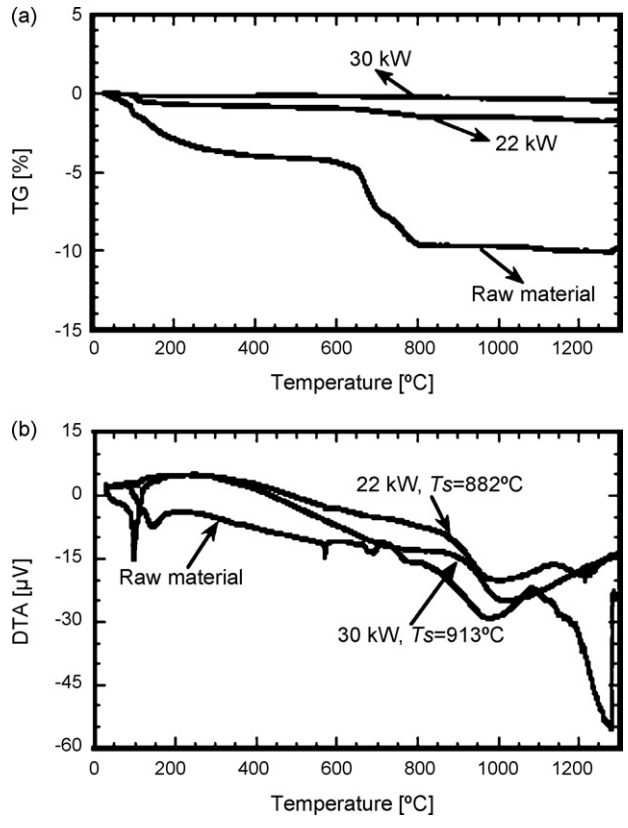

Fig. 4. TG-DTA curves of raw material and quenched powders of alkali-free glass treated by 6-phase arc with different input powers.

The thermogravimetric-differential thermal analysis (TG-DTA) was used to carry out the thermal analysis on TG-8120 (Rigaku), the measured temperature in the range of 20–1300 °C. The structures of the powders were determined by X-ray diffractometry (XRD) on Miniflex (Rigaku) with Cu Kα radiation at 30 kV and 15 mA. The data were collected in the 2θ range 3–90° with a step size of 0.02° and a scan speed of 4°/min. The micrographs of particles were performed by scanning electron microscope (SEM) on JSM5310 (JEOL) and the size distributions were evaluated by the image analysis on SEM photos. The composition of quenched powders was analyzed by inductively coupled plasma (ICP) spectroscopy on ICP-8100 (SHIMADZU).

3. Results and discussion

3.1. 6-Phase arc

Fig. 4 shows the TG-DTA analysis of alkali-free glass powders treated by 6-phase arc with different input powers. The TG curve of raw material presents two main stages with 10.1% total weight loss. In first stage, the mass loss is mainly attributed to the release of physically adsorbed H_2O and the decomposition of H_3BO_3 corresponding to the two endothermic peaks at 97

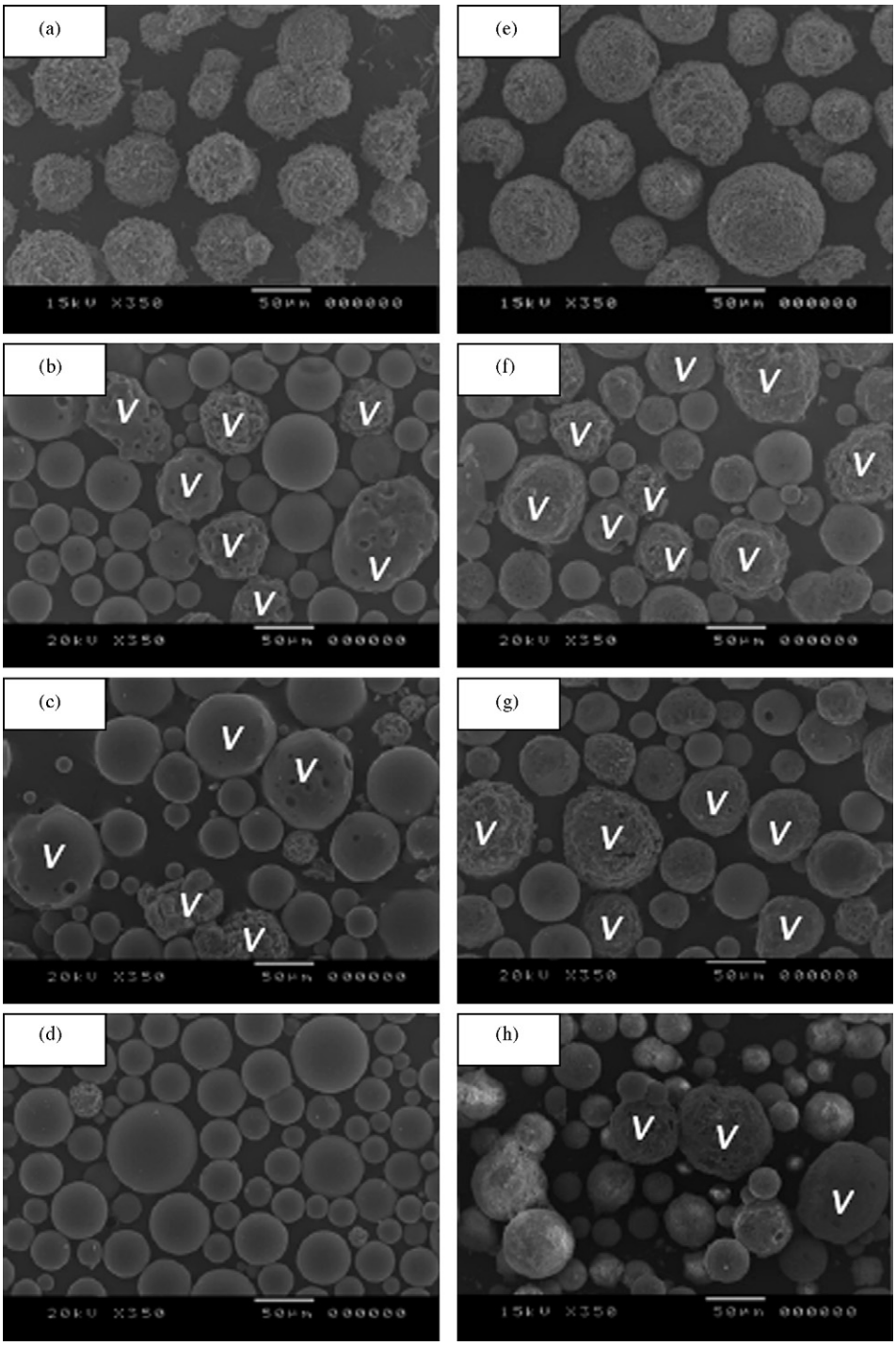

Fig. 5. SEM images of soda-lime glass powders: (a) raw material; (b) 22 kW; (c) 27 kW; (d) 30 kW, and alkali-free glass powders; (e) raw material; (f) 22 kW; (g) 27 kW; (h) 30 kW.

and 140 °C in the DTA curve. In second stage, the mass loss around 500–800 °C is due to the decomposition of $BaCO_3$ corresponding to the endothermic peaks around 680 °C. The TG curves of treated powders at 22 and 30 kW represent the smaller weight loss of 1.67% and 0.37%, their decomposition degrees are 84.3% and 96.5%, respectively. The higher decomposition degree of powders is helpful to reduce the bubbles formed by decomposed gas in molten glass to shorten the refining time. The DTA curve of quenched powders also shows a larger endothermic peak around 900 °C caused by the glass softening. Higher glass softening temperature (T_s) of powders treated with 30 kW reveals lower content of B_2O_3 which is usually used to reduce the viscosity and softening temperature of alkali-free glass.

Fig. 5 presents the SEM images of raw materials and quenched powders prepared by 6-phase arc with different input powers. The granulated particles of raw materials have rough surface and porous structure observed from Fig. 5(a) and (e). The melted particles in quenched powders look like glass beads

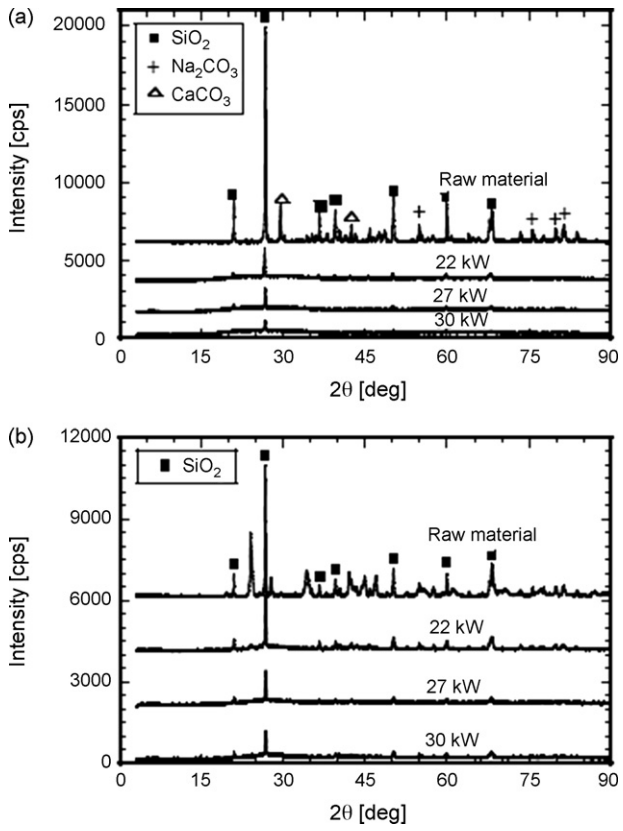

Fig. 6. XRD patterns of raw materials and quenched powders treated by 6-phase arc with different input powers: (a) soda-lime glass powders and (b) alkali-free glass powders.

which have spherical shape, smooth surface and compact structure, but some unmelted particles marked by "*V*" in samples still keep rough surface and porous structure after heating. Moreover, the surface of unmelted particles appears some small pores which were formed by the release of the decomposed gas inside particle. As the input power increases, the amount of unmelted particles decreases due to more energy transfer to particles. It is obvious that almost all particles in Fig. 5(d) melted completely in the process of in-flight melting.

To determine the structures of samples, the XRD analysis of raw materials and quenched powders treated with 6-phase arc was performed, and the results are shown in Fig. 6. It can be found that only the SiO_2 peaks appear in the patterns of treated samples, indicating that the decomposition of carbonates (Na_2CO_3, $CaCO_3$ and $BaCO_3$) or boric acid (H_3BO_3) in raw materials was almost completed in the process of in-flight melting. The peak intensity of SiO_2 in the soda-lime and alkali-free glass powders decreases with the increasing input power. The results indicate that the amount of crystal SiO_2 becomes smaller and the ratio of amorphous structure with the glass characteristics is increased.

Vitrification is a process of converting material into a glass-like amorphous solid which is free of any crystalline structure. The vitrification degree is defined as the ratio of reacted SiO_2 in quenched powders to the total SiO_2 in raw material. Fig. 7 shows the effect of input power on the vitrification degree, analyzed by the internal standard method with XRD, ZnO as standard material [19]. As the input power of arc increases, the vitrification degree of both kinds of quenched powders increases due to the higher plasma temperature caused by more energy input. The vitrification degrees of soda-lime and alkali-free glass powders are 97.8% and 82.1%, respectively at the same input power of 30 kW. The decomposition and reaction temperature of alkali-free glass raw material is higher than that of soda-lime glass raw material. According to the Ref. [20], the viscosities of soda-lime glass and alkali-free glass are 10^2 and 5.6×10^2 Pa s, respectively at 1400 °C. The removal of decomposed gas from particle inside to surface is slow under the condition of high viscosity. Hence, the vitrification degree of alkali-free glass powders is lower. The results of vitrification analysis are in agreement with the above SEM images.

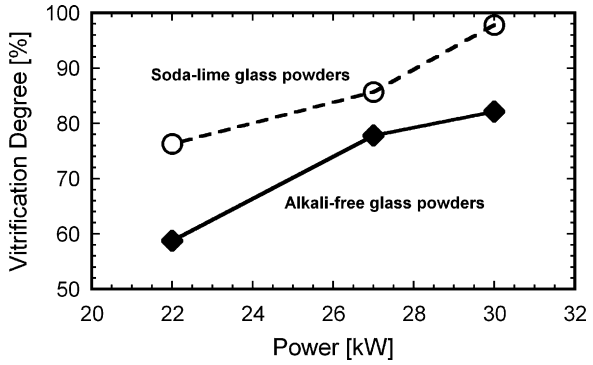

Fig. 7. Effect of input power on the vitrification of quenched powders treated by 6-phase arc.

The average diameter of quenched powders was measured and shown in Fig. 8. The particles after melting shrank due to high porosity of raw materials; the average diameter decreases with an increase in input power. The shrinkage of particle is related with its vitrification degree; higher vitrification degree results in larger shrinkage of particles. Hence, the average diameter of soda-lime glass powders at 30 kW is the smallest due to the highest vitrification. In addition, the particle size distribution of samples becomes narrower and more uniform because of higher vitrification.

3.2. 12-Phase arc

The TG-DTA curves of soda-lime glass powders treated by 12-phase arc with different input powers are shown in Fig. 9. The TG-DTA curve of raw material shows two weight loss steps: (1) the evaporation of physically adsorbed H_2O corresponding to the endothermic peak at 90 °C and (2) the decomposition of Na_2CO_3 and $CaCO_3$ corresponding to the endothermic peaks at 580 and 690 °C, respectively. However, the TG curves of quenched powders show no mass loss for both quenched powers during the treatment. It indicates that the carbonates decomposed completely during the plasma treatment in 12-phase arc. The DTA analysis shows that the sample treated at 46 kW has a higher glass softening temperature with 1039 °C. The softening temperature of soda-lime glass is mainly dependent on the Na_2O content, and more Na_2O content will lead to lower glass softening point. Also, the volatilization rate of Na_2O can

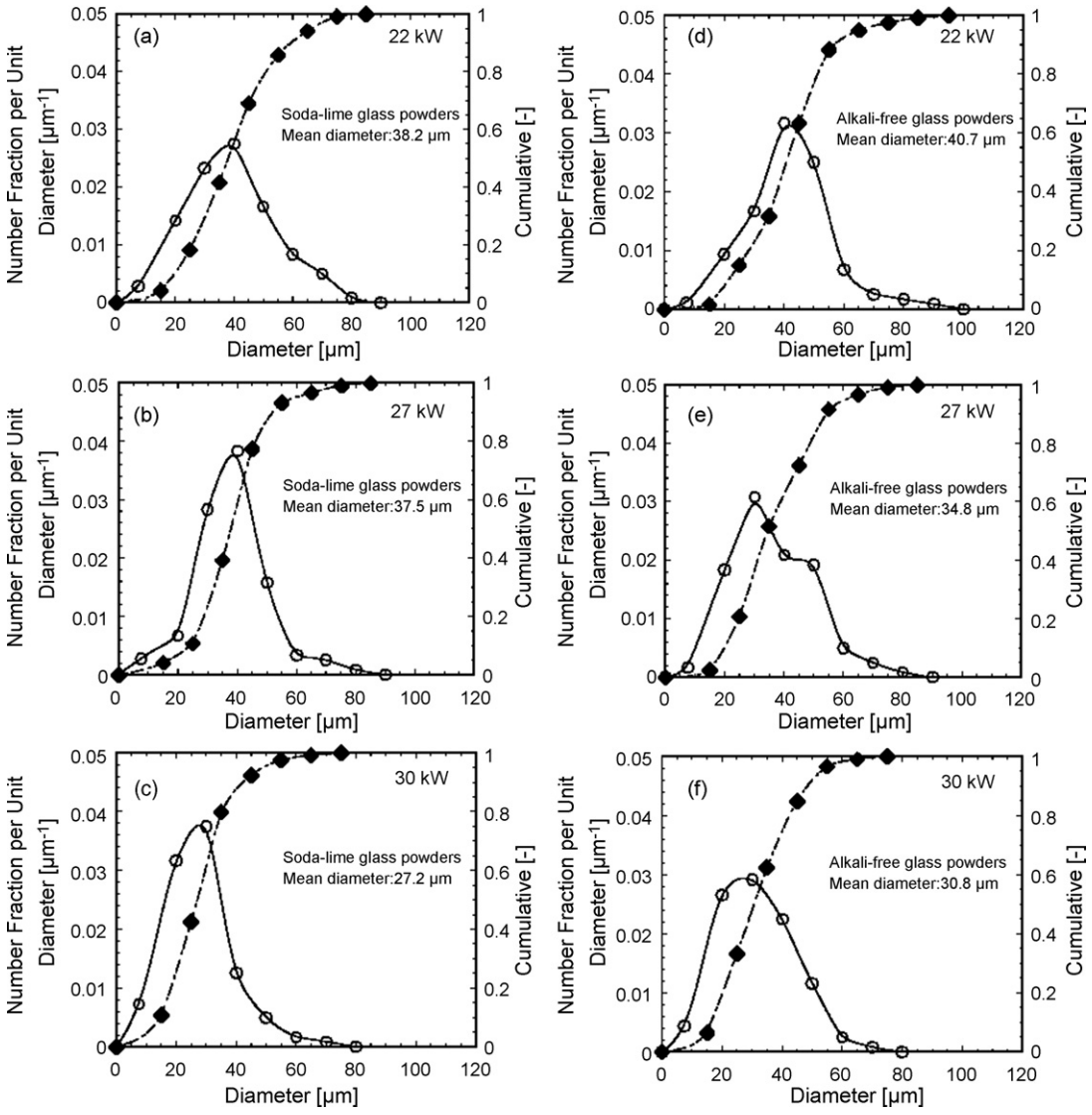

Fig. 8. Particle size distribution of quenched powders with different input powers: (a)–(c) soda-lime glass powders and (d)–(e) alkali-free glass powders.

reflect the particle temperature achieved in the process of in-flight melting. Hence, the higher glass softening temperature of powders at 46 kW predicts lower Na_2O content and higher particle temperature in sample.

In order to realize the deference between 6-phase arc and 12-phase arc, the decomposition degree of soda-lime glass powders treated by 6-phase arc and 12-phase arc are compared under the same transformer current, as shown in Fig. 10. Compared with 6-phase arc, the power of 12-phase arc is 64% and 70% higher at the input current of 100 and 125 A, respectively. Also, the volume of plasma with 12-phase arc is larger due to the usage of two layers of electrodes. Larger volume of arc plasma prolongs the residence time of particle, and more power delivered to electrodes increases the plasma temperature. Therefore, the decomposition degree of samples treated by 12-phase arc is higher than that of samples treated by 6-phase arc.

Fig. 11 shows the XRD patterns of raw material and quenched powders of soda-lime glass treated by 12-phase arc. For the quenched powders prepared at 46 kW, the pattern without any diffractive peaks reveals that the powders have whole amorphous structure with typical glass characteristics. It means the reactions among compounds were complete during the treatment. The absence of diffractive peaks of carbonates in quenched powders agrees with the above TG analysis. The quantitative XRD analysis determines that the vitrification degrees of powders treated with 36 and 46 kW are 94.5% and 100%, respectively. The residence time of injected powders is estimated about milliseconds from nozzle to collecting pan, indicating that the melting of raw material can be completed within milliseconds.

The SEM photographs of the cross-section of particles of raw material and quenched powders at 46 kW are presented in Fig. 12. As shown in figures, the particles of raw material are porous and rough, but the treated particles are compact and smooth. The measured average diameters of quenched powders are 36.1 and 33.5 μm corresponding to the power of 36 and 46 kW, respectively.

The chemical composition of soda-lime glass powders treated by 12-phase arc is given in Table 1. The CaO contents in both

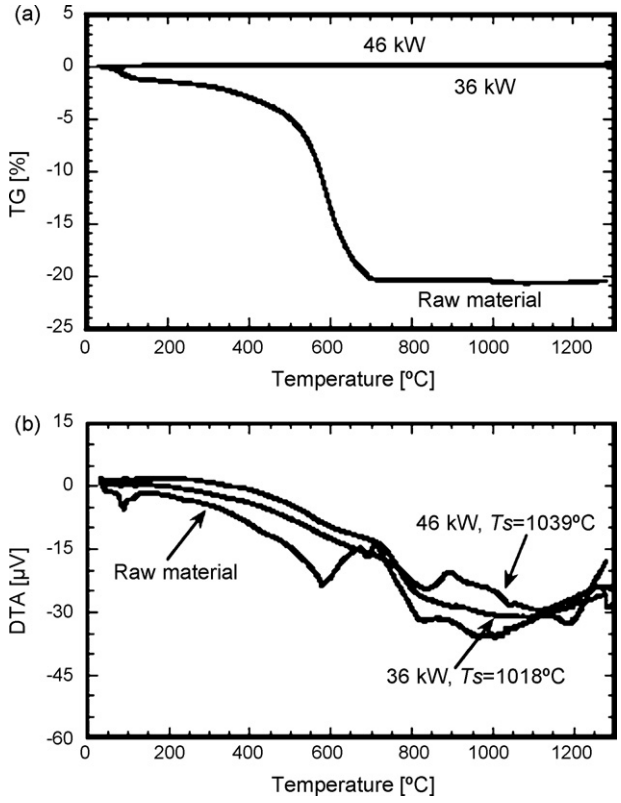

Fig. 9. TG-DTA curves of raw material and quenched powders of soda-lime powders treated by 12-phase arc with different input powers.

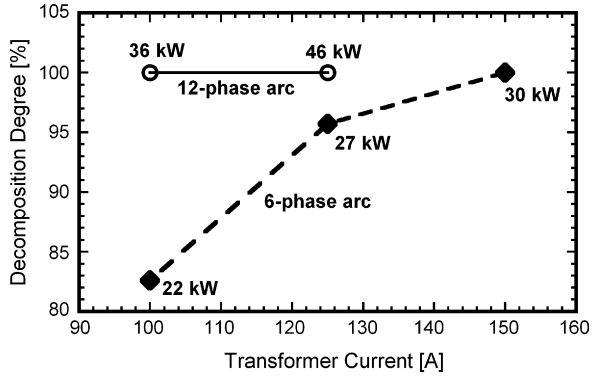

Fig. 10. Comparison of decomposition degree of soda-lime glass samples treated by 6-phase arc and 12-phase arc.

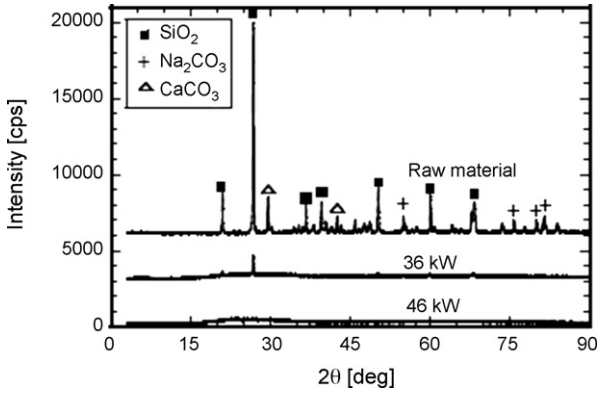

Fig. 11. XRD patterns of raw material and quenched powders of soda-lime glass treated by 12-phase arc with different input powers.

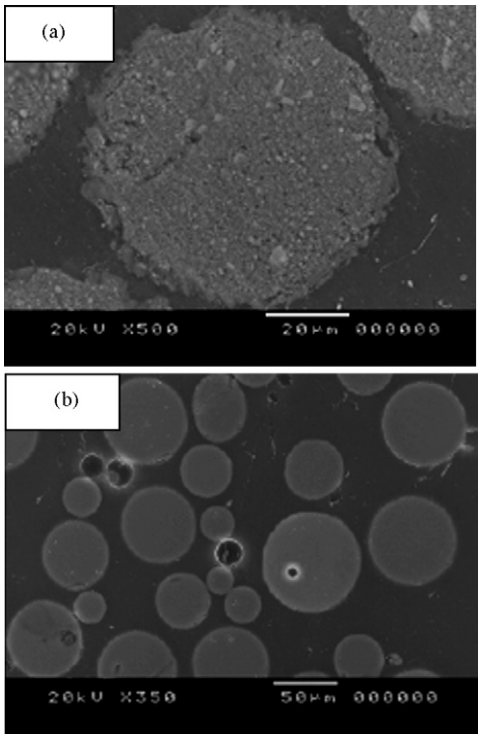

Fig. 12. SEM photographs of cross-section of soda-lime glass raw material and quenched powders treated by 12-phase arc with 46 kW.

Table 1
Chemical composition in soda-lime glass powders treated by 12-phase arc

	Composition (%)		
	Na_2O	SiO_2	CaO
Target	16.0	74.0	10.0
Sample-1 (36 kW)	12.6	77.5	9.9
Sample-2 (46 kW)	10.5	79.4	10.1

samples are close to the target, however, the SiO_2 contents are higher than that of the target. The Na_2O as an indispensable material is used to reduce the viscosity and softening temperature of soda-lime glass by controlling their content, introduced from the reagents of Na_2CO_3. The ICP composition analysis shows that the contents of Na_2O of quenched powders treated at 36 and 46 kW are 12.6% and 10.5%, respectively. Higher plasma temperature at 46 kW causes more volatilization rate of N_2O. The lower content of Na_2O in sample-2 results in higher softening temperature, which is consistent with the DTA analysis.

4. Conclusions

The multi-phase (6-phase and 12-phase) alternating current (AC) arc was successfully generated and used to melt the granulated glass raw material for the purpose of energy conservation. The influence of input power on the in-flight melting behavior of particles has been investigated. With the input power increasing, the vitrification of raw material increases because of more

energy transfer to particles; the average diameter of quenched powders decreases due to higher vitrification. Higher melting temperature and viscosity of alkali-free glass well explain the lower vitrification of raw material. The 12-phase arc provided the higher plasma temperature with larger volume and longer residence time during in-flight melting compared with 6-phase arc. The particle shrinkage in diameter is related with its vitrification; higher vitrification leads to more shrinkage of particle. The in-flight glass melting technology with multi-phase arc shortens the melting and refining time considerably.

Acknowledgements

The financial support provided by Strategic Development of Energy Conservation Technology Project of NEDO (New Energy and Industrial Technology Development Organization) is gratefully acknowledged.

References

[1] C.P. Ross, Innovative glassmelting technologies, Am. Ceram. Soc. Bull. 83 (2004) 18.
[2] T.Y. Dantsis, A.A. Zeibots, L.A. Bisnietse, M.V. Marena, S.N. Gushchin, V.B. Kutin, Improving the system of heating small glass furnaces with new burner equipment, Glass Ceram. 37 (1980) 362.
[3] K.T. Bondarev, O.N. Popov, V.A. Inshii, A.S. Bokova, Some features of the refractory lining of design elements in glass furnaces, Glass Ceram. 34 (1977) 700.
[4] V.Y. Dzyuze, Current treads in production of glass containers, Glass Ceram. 61 (2004) 101.
[5] D.E. Shamp, T.F. Stark, J.R. Elliott, L.E. Howard, Oxygen fired glass furnace with burners in the upstream end, US Patent No. 5417732, May 23, 1995.
[6] V.A. Kuzyak, Electric boosting of glass heating in flame tank furnaces, Glass Ceram. 15 (1960) 586.
[7] J. Heberlein, New approaches in thermal plasma technology, Pure Appl. Chem. 74 (2002) 327.
[8] R. Ye, J.G. Li, T. Ishigaki, Controlled synthesis of alumina nanoparticles using inductively coupled thermal plasma with enhanced quenching, Thin Solid Films 515 (2007) 4251.
[9] P. Fauchais, G. Montavon, M. Vardelle, J. Cedelle, Developments in direct current plasma spraying, Surf. Coat. Technol. 201 (2006) 1908.
[10] N.N. Rykalin, Thermal plasma in extractive metallurgy, Pure Appl. Chem. 52 (1980) 1801.
[11] T. Watanabe, M. Soyama, A. Kanzawa, A. Kanzawa, A. Takeuchi, M. Koike, Reduction and separation of silica–alumina mixture with argon–hydrogen thermal plasmas, Thin Solid Films 345 (1999) 161.
[12] M. Sakano, M. Tanaka, T. Watanabe, Application of radio-frequency thermal plasmas to treatment of fly ash, Thin Solid Films 386 (2001) 189.
[13] D. Gold, C. Bonet, G. Chauvin, A.C. Mathieu, G. Geirnaert, J. Millet, A 100-kW three phase ac plasma furnace for spheroidization of aluminum silicate particles, Plasma Chem. Plasma Process. 1 (1981) 161.
[14] S. Kumar, V. Selvarajan, P.V.A. Padmanabhan, K.P. Sreekumar, Spheroidization of metal and ceramic powders in thermal plasma jet: comparison between experimental results and theoretical estimation, J. Mater. Process. Technol. 176 (2006) 87.
[15] G. Shanmugavelayutham, V. Selvarajan, Plasma spheroidization of nickel powders in a plasma reactor, B. Mater. Sci. 27 (2004) 453.
[16] K. Matsumoto, Plasma production by multi-phase ac glow discharge at the frequency of a commercial electric power system, Plasma Sources Sci. Technol. 5 (1996) 245.
[17] J.R. Cogdell, Foundations of Electrical Engineering, Prentice-Hall, Englewood Cliffs, 1990, p. 258.
[18] T. Matsuura, K. Taniguchi, T. Watanabe, A new type of arc plasma reactor with 12-phase alternating current discharge for synthesis of carbon nanotubes, Thin Solid Films 515 (2006) 4240.
[19] D.E. Willis, Internal standard method calculations, Chromatographia 5 (1972) 42.
[20] N.P. Bansal, R.H. Doremus, Handbook of Glass Properties, Academic Press, London, 1986, p. 224.